

**ANALYSIS OF A SMITH-PREDICTOR-BASED-CONTROL CONCEPT ELIMINATING
THE RIGHT-HALF PLANE ZERO
OF CONTINUOUS MODE BOOST AND BUCK-BOOST DC/DC CONVERTERS**

Felix A. HIMMELSTOSS, Johann W. KOLAR and Franz C. ZACH

Technical University of Vienna - Power Electronics Section
Gusshausstrasse 27-29, A - 1040 Vienna, AUSTRIA
Tel. (int.+) 1 58801-3886, Fax. (int.+) 1 5052666

A B S T R A C T

As discussed in detail in the literature, the small-signal transfer function of a boost or a buck-boost converter shows a zero located in the right-half complex plane for continuous operation. This zero makes the stabilization of the system considerably difficult. This paper uses a boost converter as an example to show that application of the principle of linear prediction (as originally proposed for the control of systems with dead times) yields the mirror image of the control circuit zero. This shift of the zero into the left-half s-plane is achieved with unchanged location of the poles. Thereby the small signal transfer function is split into two parts: a phase-minimum system and a non-phase-minimum system. The latter can be interpreted as a linear Padè approximation of a dead-time element. For the design of a robust control system it is necessary to investigate the shift of the poles of the closed system dependent on the change of the operating point. Besides this it will be analyzed finally how the predictor influences the small- and large-signal system disturbance responses for changes of the load and for input voltage changes.

1. Introduction - Principle of Linear Prediction

In the following the small-signal transfer function of a boost converter is used as an example for presentation of the principle of linear prediction. For the sake of clarity the consideration of the following details shall be omitted: the influence of the ESR (equivalent series resistance) of the output capacitor and of the ohmic contribution of the inductive storage element on the control behavior. Ideal switches are assumed. This can be done because the basic dynamic system quality is not affected. The discussion of the controller design, the investigation of the robustness and the disturbance response (with respect to load and input voltage changes) will be performed in chapter two.

The derivation of the control model of a continuous mode boost converter (cf. Fig.1) leads for the small-signal behavior in the vicinity of the operating point (characterized by U_{10} , U_{C0} , I_{L0} , α_0) to the block diagram shown in Fig.2 and to a transfer function

$$S(s) = \frac{(1-\alpha_0) \cdot U_{C0}}{L \cdot C} \cdot \frac{1 - s \cdot \frac{I_{L0} \cdot L}{(1-\alpha_0) \cdot U_{C0}}}{s^2 + \frac{1-\alpha_0}{(L \cdot C)^{0.5}} \cdot \left[\frac{L}{C} \right]^{0.5} \cdot \frac{1}{R_o \cdot (1-\alpha_0)} \cdot s + \frac{(1-\alpha_0)^2}{L \cdot C}} \quad (1)$$

$$S(s) = \frac{JU_C}{J\alpha} = \frac{k \cdot (1-s \cdot T_1)}{s^2 + 2 \cdot d \cdot \Omega_0 \cdot s + \Omega_0^2} \quad (2)$$

Before the power transfer into the output side can be increased, the inductive storage element on the input side has to be charged up. This results in a system zero in the right-half s-plane or in a non-phase-minimum system behavior, respectively. This makes the circuit stabilization considerably difficult, especially for the requirement of no remaining stationary control error. Then the controller has to have an integral component. Furthermore, this system behavior can lead to an unsatisfactory dynamic behavior of the closed loop.

According to

$$S(s) = \frac{1-s \cdot T_1}{1+s \cdot T_1} \cdot \frac{k \cdot (1+s \cdot T_1)}{s^2 + 2 \cdot d \cdot \Omega_0 \cdot s + \Omega_0^2} \quad (3)$$

one can describe the control behavior of the system part between control input (point where the duty ratio is introduced into the system) and the output voltage (control response) by a combination of a first-order all-pass and a system part with phase-minimum behavior.

The interpretation of the all-pass term as a

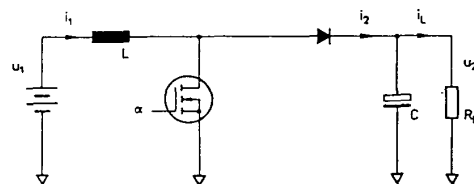


Fig.1. Structure of the power circuit of a boost converter

linear Padé approximation of a dead-time element

$$e^{-sT_e} = \frac{1 - s \cdot \frac{T_e}{2} + \left[s^2 \cdot \frac{T_e^2}{8} - \dots \right]}{1 + s \cdot \frac{T_e}{2} + \left[s^2 \cdot \frac{T_e^2}{8} + \dots \right]} \quad (4)$$

leads to the possibility of using the (appropriately modified) concept of predicting the control response by a "SMITH"-predictor.

As shown in Figs.3,4, this results in a shift of the zero (which is characteristic for continuous operation) from the right-half into the left-half s-plane. The all-pass behavior of the genuine system remains, however, as is clear from the previously described physical principle.

Therefore the controller design is performed for an equivalent system which converges to the actual system for the stationary case because the addition to the controlled system acts only in a dynamic sense.

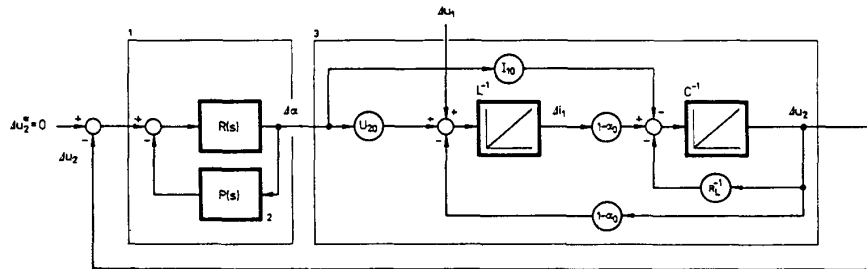


Fig.2. Structure of the control circuit of a linearized boost converter (3); prediction of the control input response of the converter by predictive controller (1)

As marked in Fig.2, this predictor adds a feedback loop to the controller showing an effect equivalent to a path parallel to the controlled system which eliminates the all-pass behavior (the "dead time"). For the transfer function of the predictor P(s) there follows

$$P(s) = \frac{k \cdot (1 + s \cdot T_1)}{s^2 + 2 \cdot d \cdot \Omega_0 \cdot s + \Omega_0^2} \cdot \left[1 - \frac{1 - s \cdot T_1}{1 + s \cdot T_1} \right]$$

$$= \frac{2 \cdot k \cdot s \cdot T_1}{s^2 + 2 \cdot d \cdot \Omega_0 \cdot s + \Omega_0^2} \quad (5)$$

A shift of the operating point corresponds to a not exact matching of the predictor to the controlled system. However, this does not lead to a limitation of the applicability of this proposed concept, as a closer analysis shows. A detailed discussion of the control robustness will be performed in section 2. There, not only the variation of the closed-loop poles dependent on the operating point will be discussed, but also the disturbance system responses due to input voltage changes and load changes. Furthermore, the small-signal disturbance responses will be analyzed in detail based on a digital simulation of the system.

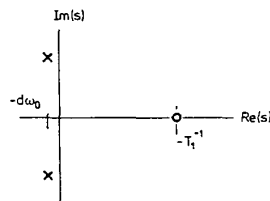


Fig.3. Pole-zero-diagram of a small-signal transfer function of a continuous-mode boost converter

Accordingly we have for the transfer function determining the stabilization and to be handled by the voltage controller R(s)

$$S(s) + P(s) = \frac{k \cdot (1 + s \cdot T_1)}{s^2 + 2 \cdot d \cdot \Omega_0 \cdot s + \Omega_0^2} \quad (6)$$

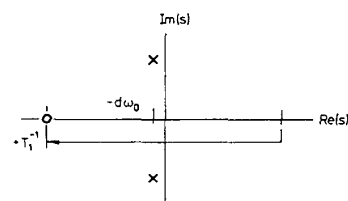


Fig.4. Pole-zero-diagram of the small-signal transfer function to be handled by the voltage controller for predictive correction of the transfer function of the converter

2. Analysis of the Control Behavior

In the following we want to investigate in more

more detail the control behavior for the example of a 12V/48V DC/DC boost converter when a predictor is used. (Such a boost converter is used, e.g. for the supply of low voltage loads from a 12V DC voltage mains buffered by a battery.) As already mentioned in chapter 1, we only want to include into the control model these components which substantially influence the system dynamics. Thereby one can clearly point out the advantages and disadvantages of a predictor control.

2.1. Parameters and Transfer Function of the Controlled System

According to the remarks made previously we assume (where the index 0 describes the operating point around which the linearization takes place):

input voltage $U_{10} = 12V$
output voltage $U_{20} = 48V$

With $L=1.8mH$ and $R_{L0} = 10\Omega \dots 100\Omega$ we have (continuous operation) for the whole load range. For the average value of the input current we have $I_{10} = 19.2A \dots 1.92A$. For the relative turn-on interval we have accordingly $\alpha_0 = 0.75$.

The value of the output capacitor is $C = 2mF$.

The small-signal transfer function of the controlled system used for the predictor becomes with Eq.(1)

$$S(s) = 192 \cdot \frac{(1 - 2.88 \cdot 10^{-3} \cdot s)}{1 + 2.88 \cdot 10^{-3} \cdot s + 5.76 \cdot 10^{-5} \cdot s^2} \quad (9)$$

$(R_{L0}=10\Omega)$

2.2. Transfer Function of the Predictor

According to Eq.(1), a shift of the operating point directly influences the dynamics of the controlled system. E.g., for a load reduction the system zero location is shifted more into the right-hand s-half-plane (its influence on the dynamics is reduced) and the damping of the polynomial of the denominator is reduced. For the predictor (which "eliminates" the effect of the system zero) we have to apply therefore the maximum load case ($R_{L0} = 10 \Omega$) because then the zero location lies closest to the origin of the s-plane; accordingly, the all-pass behavior of the controlled system is most pronounced. With Eq.(5) we have for the transfer function of the predictor

$$P(s) = 192 \cdot \frac{5.76 \cdot 10^{-3} \cdot s}{1 + 2.88 \cdot 10^{-3} \cdot s + 5.76 \cdot 10^{-5} \cdot s^2} \quad (8)$$

$(R_{L0}=10\Omega)$

2.3. Controller Design

According to Fig.2, the transfer function to be handled by the controller is given by the parallel circuit $S(s)+P(s)$ (controlled system plus predictor). As Fig.5 shows, the predictor results in a phase increase by 180° (mirror-imaging of the system zero location into the left s-half-plane, cf. Fig.4) in the upper

frequency region, as related to the phase response of $S(s)$. Thereby one can obtain a relatively high transition frequency of the open loop despite the fact that one has to incorporate an I-term into the controller for sufficient accuracy in the stationary case. The frequency response of the open loop is shown in Fig.6 (phase margin 70°) as result for using a PI-controller

$$R(s) = 0.0946 \cdot \frac{(1 + 7.59 \cdot 10^{-3} \cdot s)}{7.59 \cdot 10^{-3} \cdot s} \quad (9)$$

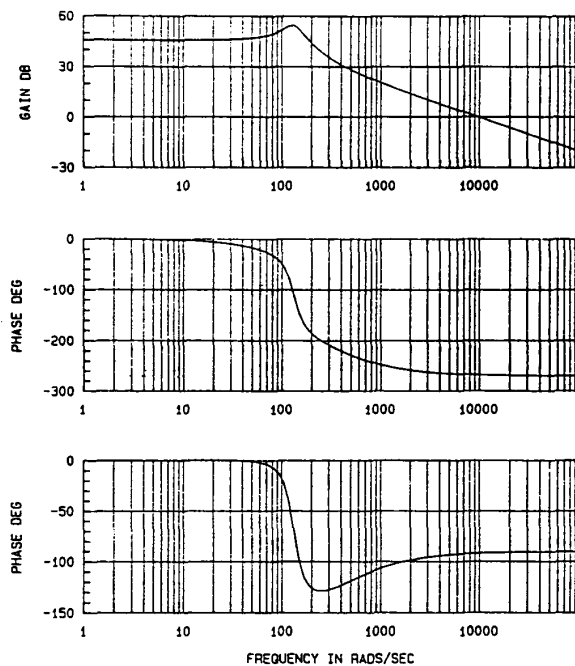


Fig.5. Bode plot of the controlled system
upper curve: gain of $S(s)$ and $S(s)+P(s)$
middle curve: phase of $S(s)$
lower curve: phase of $S(s)+P(s)$

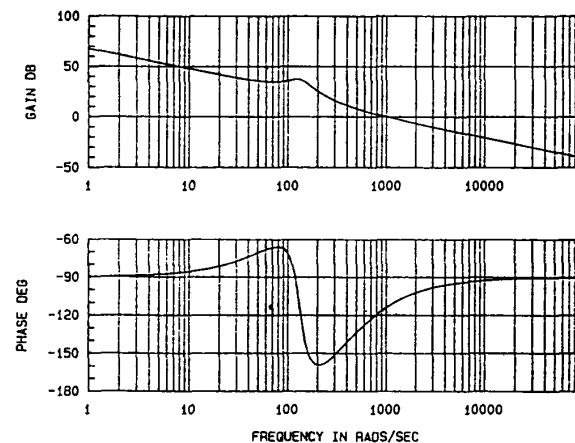


Fig.6. Bode plot of the open control loop ($S(s)+P(s)$ in series with PI-controller $R(s)$)

The determination of the controller gain and of the integration time can, under consideration of the limited controller output region, be performed also by using the root locus diagram (cf. Fig.7), besides using the Bode diagram. The branches of the root locus diagram are drawn to the left via the mirror-image of the system zero location. Therefore, for the simple model chosen here, stable behavior of the closed loop circuit is given independently of the controller gain.

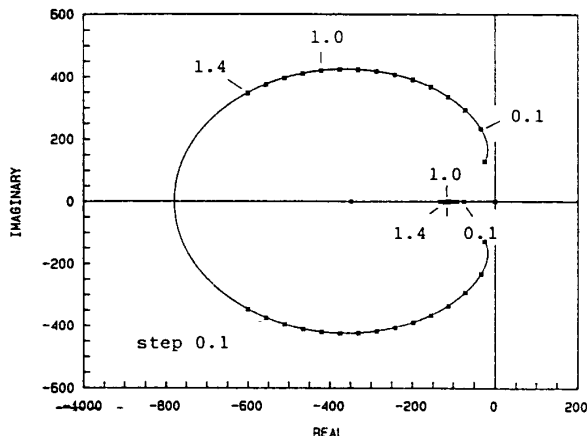


Fig.7. Root locus diagram for $R_{L0} = 10\Omega$, system to be controlled $S(s)+P(s)$ with PI controller

2.4. Reference Value Response

For investigation of the reference value response of the control we apply an output voltage reference value step of $\Delta u_c^* = 1V$. The reaction of the linear system (cf. Fig.8) corresponds to a high degree to that of the nonlinear system. Therefore, the representation of the nonlinear system can be omitted here.

As one could expect, a reduction of the output voltage appears before an increase as caused by the all-pass behavior. However, the controller "gets the impression" of an immediate output voltage increase according to the additive supplement of the controlled system response by the predictor ("compensation" of the all-pass behavior).

For checking the robustness of the predictor control we want to investigate furthermore a reference value step for $R_{L0}=100\Omega$ (minimum output load), cf. Fig.9. As already mentioned in section 2.2, then the all-pass behavior effect is largely reduced. As Fig.10 shows, despite to the fact that the predictor is not matched to the controlled system any more (because it has been designed for $R_{L0}=10\Omega$), all poles and zeroes of the open loop lie in the left-hand s-plane. For the controller gain as chosen in section 2.3 we still have stability. However, predictor $P(s)$ and controlled system $S(s)$ show different polynomials of the denominator in this case. This leads to a split of the poles of $S(s)+P(s)$ into two conjugate complex poles and a closely neighbouring conjugate complex zero or to a conjugate complex pole pair (lying close to the imaginary axis)

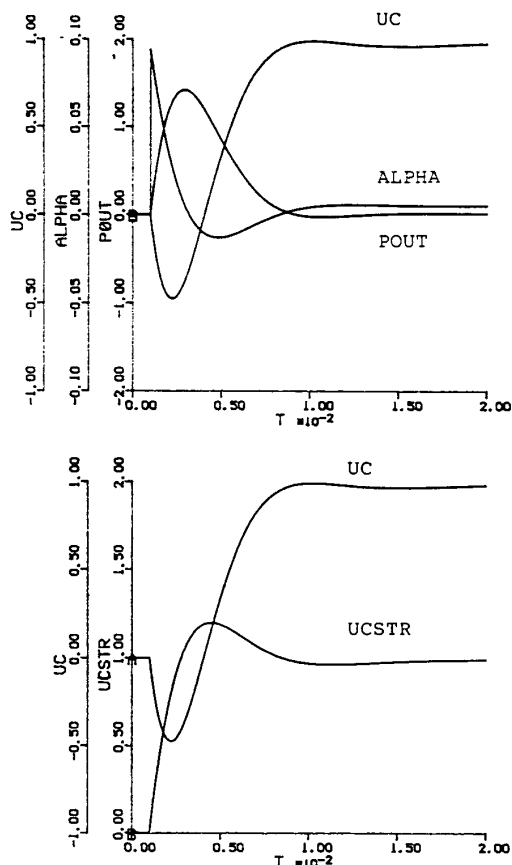


Fig.8. Step response of the closed system due to a voltage reference value step of 1V ($R_{L0} = 10\Omega$)
UC...output voltage
ALPHA...duty cycle α (controller output)
POUT...predictor output
UCSTR...sum of predictor output and output voltage

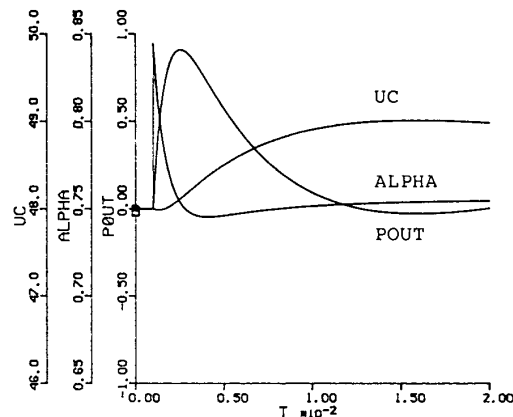


Fig.9. Step response of the closed system due to a voltage reference value step of 1V ($R_{L0} = 100\Omega$)
UC...output voltage
ALPHA...duty cycle α (controller output)
POUT...predictor output

of the closed loop which results in a little damped oscillation of the capacitor voltage (cf. Fig.10).

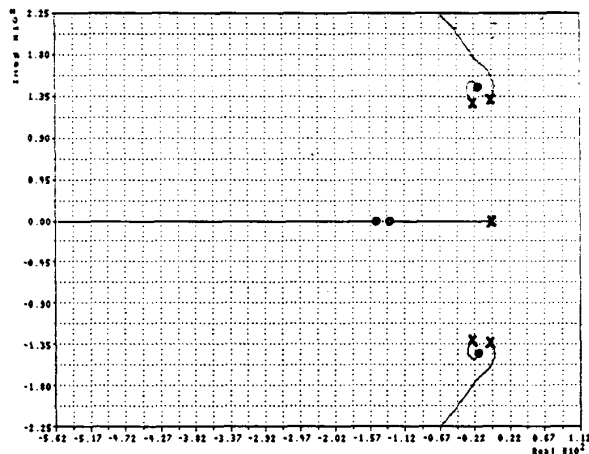


Fig.10. As Fig.7, but for $R_{L0} = 100\Omega$

2.5. Disturbance Response

The disturbance response of the control (i.e., the behavior regarding to input voltage and load changes) is analyzed based on the calculation of the system reaction following an input voltage step (cf. Fig.11) or a load step (cf. Fig.12).

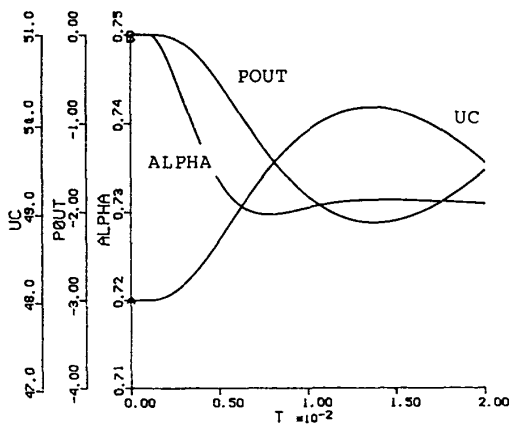


Fig.11. Step response due to a load step of +10% ($R_{L0} = 10\Omega$)

In both cases one can see that the applicability of the predictor (which has been designed for predicting of the system response due to a reference value change at the input of the controlled system) is only very limited for handling of disturbances acting inside of the controlled system.

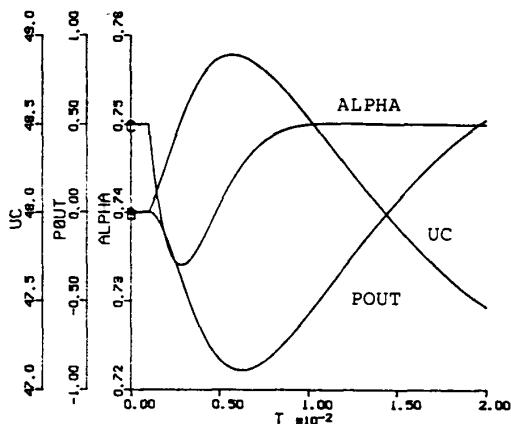


Fig.12. Step response due to a input voltage step of +10% ($R_{L0} = 10\Omega$)

For the conditions given here, after a short controller reaction, the predictor and controlled system outputs oscillate with opposite phases and therefore do not appear in the controlled variable (formed as summation of both signals). The weakly damped decay behavior of the oscillation therefore is determined by the poles of the open (and not of the closed) loop. As Fig.13 shows ($\Delta R_L = 10\Omega$), this behavior occurs also for mismatch of the predictor (designed for $R_{L0} = 10\Omega$) and of the controlled system.

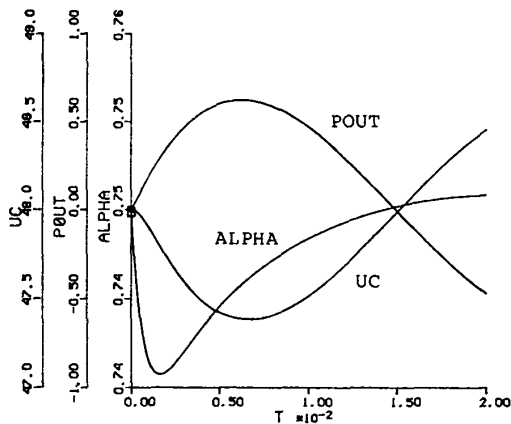


Fig.13. Step response due to a load step of -10% ($R_{L0} = 100\Omega$)

3. Conclusions

Aim of this paper has been to present the concept of a predictor control and to point out limits of its applicability. For practical realization, of course, $R(s)$ and $P(s)$ will be combined into one controller transfer function

$$R^*(s) = \frac{R(s)}{1+R(s) \cdot S(s)} \quad (10)$$

and they will not be realized separately. Besides the prediction of the controller output response of the controlled system also a prediction of the disturbance response of the controlled system can be performed. This concept which substantially improves the behavior of the controlled system regarding disturbances and the considerations regarding the general robust design of predictor controls will be the subject of a future paper.

Finally, we want to present briefly the behavior of the control loop without predictor. For obtaining stable operation we have to decrease the controller gain by 40dB there. The controller dynamics thereby is worsened considerably (cf. Fig.14, reference value step response $\Delta u_c^* = 1V$); the comparison with Fig.8 clearly shows the advantages given for predictor control.

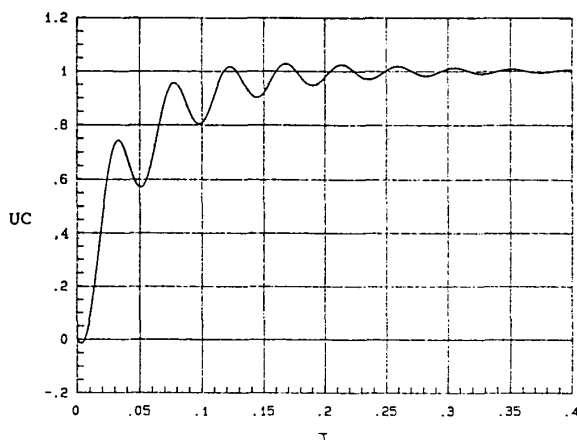


Fig.14. Step response of the closed system without predictor due to a reference value step ($\Delta u_c^* = 1V$, $R_{Lo} = 10 \Omega$, Controller gain reduced by 40dB)

- [7] Smith, O.J.M.: Feedback Control Systems. McGraw-Hill Series in Control Systems Engineering, New York, Toronto, London. 1958.
- [8] Weinmann, A.: Die bestimmte und verallgemeinerte Vorhersage von Signalen in linearen Regelsystemen. Elin-Zeitschrift 17, H.1/2, pp.18-55.1965.
- [9] Schmidt, G.: Vergleich verschiedener Totzeitregelsysteme. Messen-Steuern-Regeln 10, H.2, pp.71-75. 1967.
- [10] Frank, P.M.: Vollständige Vorhersage im stetigen Regelkreis mit Totzeit. Regelungstechnik 16, H.3, pp.111-116, pp.214-218. 1968.

ACKNOWLEDGEMENT

The authors are very much indebted to "Siemens AG Österreich", especially the Switched Mode Power Supply Section, who supports the work of the Power Electronics Section at their university.

REFERENCES

- [1] Middlebrook, R.D., and S.Cuk: Advances in Switched-Mode Power Conversion, Vol.1. Pasadena: Teslaco. 1981.
- [2] Amanuma, K., Naruke, K., and Sakaki, Y.: Optimal Control for Electromagnetic Power Supply. PESC'88, Kyoto, April 88, pp.369-376.
- [3] Matsuo, H., F.Kurokawa, T.Tauchi and H.Sako: Dynamic Characteristic of the Digitally Controlled DC-DC Converter. PESC'88, Kyoto April 88, pp.997-1004.
- [4] Lee, F.C. and D.J.Shortt: An Improved Model for Predicting the Dynamic Performance of Wide-Bandwidth Switching Converter. Proceedings of Powercon 11, 1984. pp. E-3 1-14.
- [5] Himmelstoss, F.A. and F.C.Zach: State space control for a step-up converter. IEEE INTELEC'1991, Kyoto, Nov.6-8, 1991.
- [6] Himmelstoss, F.A., J.W.Kolar, and F.C.Zach: Comparison of Control Structures for a Bidirectional High-Frequency DC-DC Converter, Proceedings of the European Space Power Conference, Madrid Oct. 2-6, 1989, pp.403-408.